

Energy dispersive X-ray fluorescence methodology and analysis of suspended particulate matter in seawater for trace element compositions and an intercomparison with high-resolution inductively coupled plasma-mass spectrometry

Nathaniel J. Buck ^{1,2,3,*} Pamela M. Barrett ^{1,2} Peter L. Morton ⁴ William M. Landing ⁵
Joseph A. Resing ^{1,2,3}

¹Joint Institution for the Study of the Atmosphere and Ocean, University of Washington, Seattle, Washington

²Cooperative Institute for Climate, Ocean, and Ecosystem Studies, University of Washington, Seattle, Washington

³NOAA/Pacific Marine Environmental Laboratory, Seattle, Washington

⁴National High Magnetic Field Laboratory, Geochemistry Group; and the Department of Earth, Ocean and Atmospheric Science, Florida State University, Tallahassee, Florida

⁵Department of Earth, Ocean and Atmospheric Science, Florida State University, Tallahassee, Florida

Abstract

A modification of energy dispersive X-ray fluorescence (ED-XRF) for analysis of trace element concentrations in suspended particulate matter (SPM) in seawater and intercomparison with high-resolution inductively coupled plasma-mass spectrometry (HR ICP-MS) is presented. Approximately 250 SPM samples were collected on polycarbonate track-etched filters in the Indian Ocean during the U.S. CLIVAR/CO₂ Repeat Hydrography meridional section I09N cruise in 2007. Samples were first analyzed by ED-XRF, a nondestructive technique, for Al, P, Ti, Mn, Fe, Ni, Cu, and Zn and subsequently digested and quantified by HR ICP-MS, creating two blind, basin-scale data sets used for a paired statistical comparison. Our results found (1) ED-XRF analysis using thin-film principles can quantify the elemental composition of SPM at nanomolar concentrations found in the open ocean; (2) there was excellent agreement between ED-XRF and HR ICP-MS analyses for Al, Fe, and Mn and good agreement for P and Ti; (3) analytical differences were the largest for Cu, Ni, and Zn; (4) HR ICP-MS methods have lower detection limits for most elements when compared to the ED-XRF; (5) ED-XRF analysis has a closer agreement to reported values for the NIST SRM 2783 standard and lower relative standard deviations when compared to the HR ICP-MS. We recommend continued refinement of nondestructive ED-XRF methods as this would allow for the easy exchange of filtered samples between lab groups for intercalibration and intercomparison of basin-scale hydrographic cruises and archival for future analysis.

The distribution and elemental composition of suspended particulate matter (SPM) in the oceans reflect patterns of atmospheric, fluvial, and hydrothermal inputs as well as biological uptake, particle scavenging, and vertical transport through the water column. Particles have a preeminent influence on the marine biogeochemical cycle of trace elements and their isotopes (TEIs). Particulate scavenging and dissolution processes determine chemical and physical speciation (Lam et al. 2015), residence times of the dissolved fraction (Jeandel et al. 2015), and vertical export rates for many TEIs (Lamborg et al. 2008a,b). Thus,

quantifying chemical compositions and distributions of marine suspended particulates is crucial to understanding the biogeochemical cycling of trace elements in the oceans. However, while SPM is important to the geochemistry for a wide array of elements, a comprehensive understanding of particulate chemistry in the marine environment has not been realized, due mainly to the absence of robust, calibrated, and thoroughly tested methods for TEIs sample collection and analysis (Jeandel et al. 2015).

Energy-dispersive X-ray fluorescence (ED-XRF) methods for the analysis of marine particulate matter in estuarine and continental slope environments were originally developed in the 1970s (Baker 1976; Baker and Piper 1976; Feely et al. 1991). It is a nondestructive method that requires little sample preparation or treatment and can quantify most elements with an atomic mass greater than 11. These methods have been used in prior work to study trace element compositions and distributions of SPM

*Correspondence: nathan.buck@noaa.gov

Additional Supporting Information may be found in the online version of this article.

associated with hydrothermal venting (Feely et al. 1987, 1991, 1998; Resing et al. 2009); SPM in the upper water column of the North Atlantic (Barrett et al. 2012, 2015) and Indian oceans (Barrett et al. 2018); and aerosols collected in the marine atmospheric boundary (Buck et al. 2010*a,b*, 2013). High-resolution inductively coupled plasma-mass spectrometry (HR ICP-MS) is another technique frequently used for trace element analysis of marine particulate matter. In this method, SPM loaded onto a filter are leached or digested to a soluble phase then analyzed by ICP-MS (Cullen et al. 2001; Krachler 2007; Bowie et al. 2010; Planquette and Sherrell 2012; Lam et al. 2015). ICP-MS analytical procedures usually report limits of detection in the pmol L^{-1} range for many elements. However, poor digestion efficiencies and filter blanks can introduce larger uncertainties for some elements (Bowie et al. 2010; Planquette and Sherrell 2012).

The goal of this study is to advance marine biogeochemical studies, and the GEOTRACES mission specifically, by presenting an intercomparison of two methods used to determine the elemental composition of particulate matter in seawater at nanomolar concentrations. GEOTRACES is an international program dedicated to the sampling, analysis, and study of TEIs and has focused attention on: inputs and processes that influence TEIs in the ocean; developing standard reference materials (SRMs) that have concentrations representative of the open ocean for use in methodological ground truthing; the intercalibration of analytical methods and sampling techniques used between laboratories; and addressing the scarcity of marine particulate TEIs data sets (Anderson and Hayes 2015). For this evaluation, we analyzed 252 SPM filter samples for Al, P, Ti, Mn, Fe, Ni, Cu, and Zn in duplicate using ED-XRF followed by a total chemical digest and ICP-MS analysis. The choice of analytes represents essential micronutrients (Fe, Mn, Cu, Zn) and commonly used tracers for major particle compositions (Al, P, Ti), internal particle cycling (Mn, Fe), and external TEI inputs (Al, Mn, Fe, Ti, Ni, Cu, Zn). We then compared and contrasted the paired results with nonparametric and orthogonal distance regression statistical methods, which allowed us to identify systematic errors and bias between the two techniques. Additionally, this study describes the adaptation of ED-XRF methodologies for the analysis of marine suspended particulate matter from open-ocean environments with low trace element concentrations. To accomplish this, it was necessary to develop low-level ED-XRF calibration standards to improve detection limits for particulate Fe and Mn.

Materials and procedures

Sample collection

Marine SPM samples were collected from the upper 1000 m of the Northern Indian Ocean on the U.S. CLIVAR/CO₂ Repeat Hydrography meridional section I09N cruise in 2007 between approximately 2–18°N and 86–92°E (see Supporting Information Fig. S1A,B for station locations and depth distributions). Details on sampling protocols, dates, locations, and depths as well as geological setting and background can be found in Barrett et al. (2018). Briefly, seawater was collected using 12-liter GO-FLO

bottles mounted on a trace metal-clean rosette from the surface to 1000 m and processed in a clean laboratory van equipped with a high efficiency particulate arrestance (HEPA) filtered air system (Measures et al. 2008). Suspended particulate matter was collected by pressure-filtering (< 55 kPa, filtered compressed air) seawater through acid-washed, 0.4 μm track-etched, polycarbonate filters, backed with mixed cellulose ester filters to facilitate even sample loading, in polypropylene filter holders. The average filtration volume was 8.8 ± 2.2 L. Filters were rinsed with ~ 15 mL of ultrapure (UHP; 18.2 M Ω -cm) water adjusted to pH 8 with ammonium hydroxide, with a low vacuum applied to remove residual sea salt while avoiding loss or redistribution of particles. While this gentle rinsing might result in a minor modification of the marine SPM composition (e.g., lysing of biogenic particles by osmosis; Twining et al. 2015), removing the high salinity matrix is necessary to avoid ED-XRF artifacts resulting from the major cations and anions (chlorine interferes with P, S, K, and Ca making quantification of these elements impossible).

ED-XRF analysis

In ED-XRF methods, excitation X-rays from a source tube irradiate an analyte sample of SPM deposited on a filter, generating fluorescence X-ray energies characteristic of each element. These fluorescent X-rays are collected with a semiconducting detector and are converted into electrical voltage pulses that can be measured electronically. Quantitative ED-XRF analysis is a comparative technique; thus, the intensity of a fluorescence X-ray of an element from a sample must be compared to standards of known concentrations. As only small masses of diluted suspended material are produced by filtering of 2–10 L of open ocean seawater, XRF thin-film principles are applied, which allow for analysis of a sample using as little as 30 μg of particulate material. Fluorescent radiation intensity is strongly dependent on sample composition, particle size, excitation conditions, and instrumental parameters; two criteria must be met to apply thin-film methods to particle analysis (Holmes 1981; Quisefit et al. 1994). First, particle loadings must be deposited as a uniform layer on the filter membrane. Second, the thickness of the SPM sample must be “thin” relative to both the penetration depth (the length to which a primary X-ray can penetrate) and effective layer thickness (the depth from which a fluorescent X-ray can emerge) of the characteristic X-rays for the elements of interest. This ensures the intensity of measured fluorescence X-rays are a function of the elemental mass of each sample and thus avoids matrix effects such as enhancement and absorption. Theory holds that sample thickness should be approximately $< 1/5$ the fluorescent wavelength to eliminate these effects (for reference, penetration depths for K-alpha energies for elements of interest are in the order of 5–50 μm).

Standards prepared from thin-film deposits of certified geochemical reference materials have been successfully used for ED-XRF calibration in previous reports (Feely et al. 1991). In this approach, a known quantity of SRM, of a similar matrix (i.e., U.S. Geological Survey Standard Sediment and Rocks MAG-1, GRX-1, -4, and -6), is suspended in a pH-adjusted solution and then loaded

onto the same filter type used for sample acquisition. However, at small masses, heterogeneity in reference materials decrease the precision of replicate analyses (Kurfurst 1991; Kurfurst et al. 1993; Pauwels and Vandecasteele 1993). Additionally, many solid reference material certifications report a “minimum recommended mass” between 100 and 200 mg be used to ensure a homogenized sample. For example, BCR-414 (phytoplankton; European Commission 2017) and PACS-2 (marine sediment; National Research Council of Canada 1997) have certified minimum sample sizes of 100 mg and 250 mg, respectively. To maintain thin-film assumptions, the critical filter loading mass (the limit above which the relationship between counts and weight is nonlinear) for a 37 mm filter is $\sim 1600 \mu\text{g}$, an order of magnitude lower than the certified value for many options for appropriate reference materials. There is also concern that selective dissolution of individual elements may occur when the sample is suspended for filtration onto the filter, introducing additional uncertainties. To this point, Buck et al. (2013) found the median fractional solubility of Pacific Ocean aerosols to be 6.4% for Fe, 3.7% for Al, and 45.1% for Mn. To avoid these potential complications, calibrations for all

elements were performed using commercially available thin-film standards (MicroMatter). Furthermore, to accurately measure the low particulate Fe and Mn concentrations typically present in open-ocean surface seawater samples ($< 5 \text{ nmol L}^{-1}$), the minimum determination limit of the ED-XRF was improved with the addition of low-concentration calibration standards ($< 1000 \text{ ng cm}^{-2}$) prepared in-house using a modification of a method reported by Holynska and Bisniek (1976) that employs diethyldithiocarbamate (DDTC) to quantitatively precipitate trace metals from a solution of known concentration (Fig. 1). A thorough description of low-level standard preparation can be found in the Supporting Information. Briefly, known concentrations of DDTC-Fe and DDTC-Mn precipitates made with commercially available dissolved Fe and Mn standard solutions were loaded onto cleaned polycarbonate track-etched (PCTE) filters (47 mm diameter, $0.4 \mu\text{m}$ pore size). Standard preparation procedures were optimized for solution DDTC : Fe and DDTC : Mn ratios as well as incubation (shaking) time with respect to XRF count intensity (Supporting Information Figs. S2, S3). Accuracy of the method was established by digestion and graphite furnace absorption

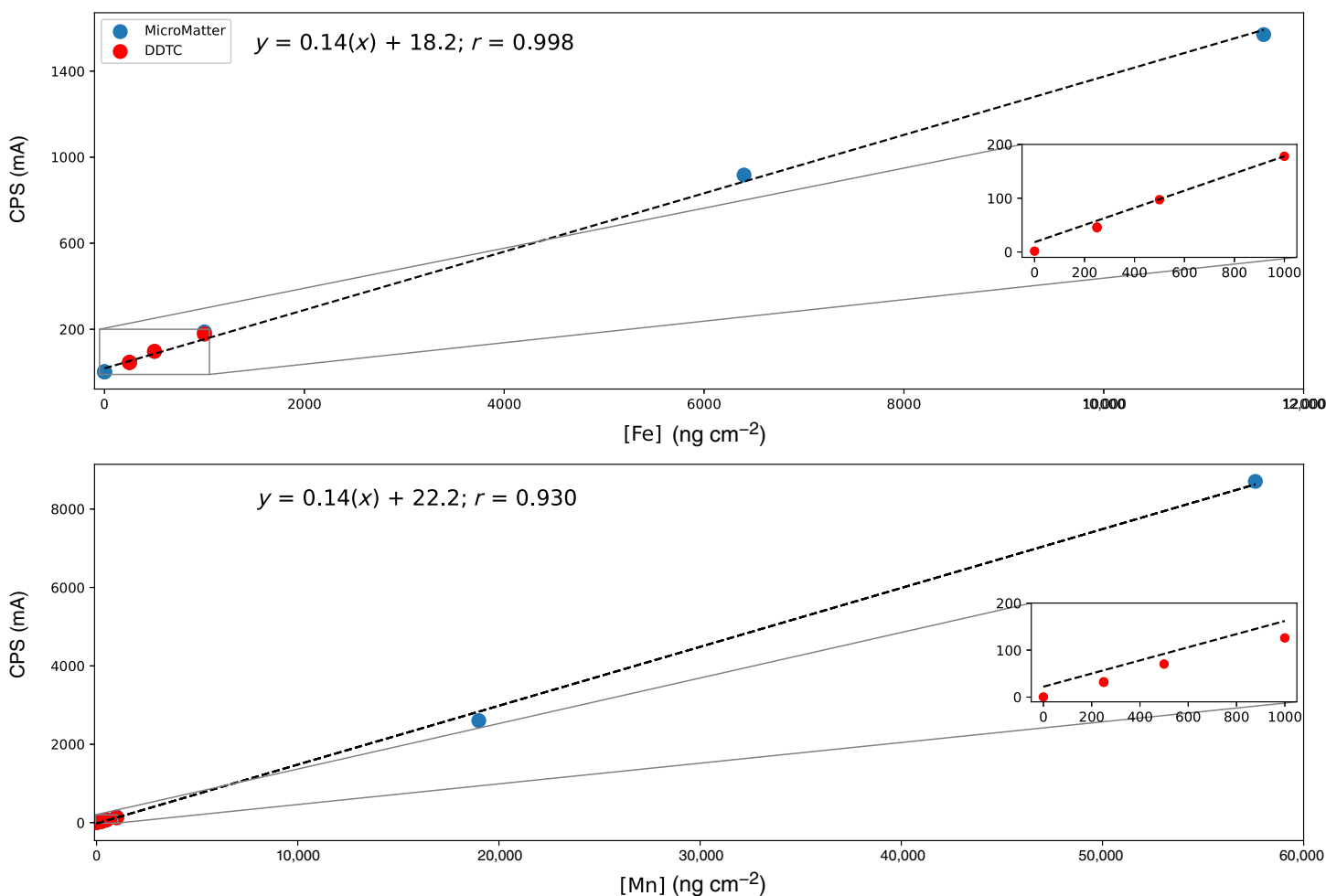


Fig 1. ED-XRF standard curve for Fe and Mn. Blue circles represent commercially available MicroMatter calibration standards. Minimum determination limits were improved with the addition of low concentration calibrants fabricated with a DDTC precipitate method (red circles).

spectrometry analysis (Supporting Information Fig. S4). Furthermore, scanning electron images found a layer of evenly distributed particles, verifying that standards satisfy thin-film criteria. Particles on prepared DDTc standards were approximately the same size (1–10 μm) as SPM found in the upper ocean (lithogenic aerosols, small phytoplankton, detritus; Buck et al. 2010a; Supporting Information Fig. S5).

The trace element composition of SPM sample filters was first analyzed by ED-XRF at the NOAA/Pacific Marine Environmental Laboratory in Seattle, Washington. ED-XRF analysis was conducted under a vacuum atmosphere using thin film principles on a Thermo Fisher Quant'X equipped with a Rhodium Target X-Ray tube and an electronically cooled, lithium-drifted solid-state detector. X-rays for primary sample excitation were passed through graphite and metal filters for optimum control of peak-to-background ratios (Ellis 2001). Excitation conditions for each analyte can be found in Table 1. Four separate QA/QC procedures are conducted on a daily, weekly, and monthly basis. First, a daily energy adjustment is performed for an energy channel alignment of the Quant'X. Second, ongoing weekly calibration verification is run using a series of multielement samples to monitor machine drift. Reference material NIST 2783 is also analyzed on a weekly basis to monitor recovery of individual elements. Last, a monthly analysis of 10 acid-washed blank filters is run for accurate background determination and monitoring.

Filter digestion and ICP-MS analysis

While sample processing methods for ICP-MS vary slightly among research groups, several recent intercomparison exercises demonstrate that the concentrations of major and trace elements in marine SPM can be quantitatively and reproducibly determined using a minimum “best practice” set of procedures (Planquette and Sherrell 2012; Ohnemus et al. 2014; Twining et al. 2015). Typically, filtered marine SPM is subjected to a strong acid digestion, including nitric acid (HNO_3 ; and possibly hydrogen peroxide, H_2O_2) to dissolve the authigenic and organic

Table 1. ED-XRF excitation conditions for trace elements of interest. The composition of suspended particulate matter was analyzed at the Pacific Marine Environmental Laboratory in Seattle, Washington. ED-XRF analysis was conducted under a vacuum atmosphere using thin-film principles on a Thermo Fisher Quant'X equipped with a Rhodium Target X-Ray tube and an electronically cooled, lithium-drifted solid state detector. X-rays for primary sample excitation were passed through graphite filters for optimum control of peak-to-background ratios.

Condition	Filter	Voltage (kV)	Current (mA)	Analytes
Low Za	Graphite thin	10	1.98	Al, P
Mid Za	Pd thin	30	1.66	Ti, Mn, Fe, Ni, Cu, Zn

components of the bulk material, and hydrogen fluoride (HF) to dissolve the lithogenic components, for example, Ti and Zr-containing minerals in samples collected from surface, coastal, and nepheloid zones (Eggemann and Betzer 1976; Cullen and Sherrell 1999; Ho et al. 2011; Ohnemus et al. 2014) followed by heating at ~ 120 – 140°C for three or more hours to digest both SPM and the filter substrate (Cullen and Sherrell 1999; Ohnemus and Lam 2015; Morton et al. 2019). Alternatively, the total digestion of the filter substrate and marine SPM can be achieved efficiently using a microwave accelerated digestion system, which subjects the filtered sample to both heat and pressure (Ho et al. 2011). All heating methods then cycle the digest solutions one or more times through a series of drydowns and digestion steps using HNO_3 (and optionally H_2O_2) to fully digest the organic filter material and produce a matrix suitable for direct analysis by ICP-MS (e.g., $0.32 \text{ mol L}^{-1} \text{ HNO}_3$, a.k.a. “2% HNO_3 ”). Concentrations of major and trace elements are then determined by comparison against a calibration curve of multielement external standards, with matrix effects and instrumental drift accounted for by spiking each sample quantitatively with a constant concentration of an internal standard (e.g., In, Sc, Y). To validate the procedural digestion efficiencies, reference materials of marine sediments, plankton, and/or aerosol dust are subjected to the same digestion procedures and analyzed.

After the I09N SPM filters were analyzed by ED-XRF, they were shipped to Florida State University (FSU) for total digestion and analysis by HR ICP-MS. All work at FSU was conducted in a Class-1000 clean lab in the Geochemistry division of the National High Magnetic Field Laboratory, according to methods detailed in Morton et al. (2013). In brief, filter samples were folded twice (into quarters) and placed into acid-washed 20-mL microwave digestion jars with 3.8 mL concentrated HNO_3 (16 mol L^{-1} , quartz distilled) and 0.2 mL concentrated H_2O_2 (30%, Fisher Optima). The samples sat loosely capped in an exhausting hood overnight, to allow the escape of any gases produced by easily oxidizable organic matter. An additional 1.4 mL of concentrated HNO_3 (16 mol L^{-1} , quartz distilled) and 0.8 mL of concentrated HF (32 mol L^{-1} , Teflon distilled) were added to the microwave digestion vials, and the samples were then tightly capped and microwaved (CEM Mars Xpress) at 180°C and 1200 W for 30 min after a ramp time of 10 min. The PCTE filters completely digested and dissolved, and the resulting digest solutions were transferred to 15-mL Savillex Teflon beakers. The microwave vials were then rinsed twice with 2-mL of UHP water, into the Savillex beakers. The digest solutions were heated uncapped at 80°C overnight on an enclosed double HEPA-filtered laminar flow hotplate (flowbox) to evaporate the acids and produce a small digest residue droplet. Finally, the digest residues were redissolved in 5 mL $0.32 \text{ mol L}^{-1} \text{ HNO}_3$ (quartz distilled), by tightly capping the jars and heating on the flowbox hotplate for 30 min at $\sim 135^\circ\text{C}$. The samples were then spiked with 10 ppb In (High Purity Standards, Charleston, South Carolina) as an internal standard to account for instrumental effects and stored in

acid-washed 15-mL polypropylene centrifuge tubes until ICP-MS analysis, which usually occurred within 3–5 d of digestion.

Concentrations of major and trace elements were quantified using 7-point external calibrations (0–500 ppb) prepared from a multielement standard (High Purity Standards, Charleston, South Carolina). The digest solutions were introduced through a 200 $\mu\text{L min}^{-1}$ PFA-ST nebulizer (Elemental Scientific) and Teflon spray chamber (Savillex) into the Thermo ELEMENT2 HR ICP-MS. All elemental counts were normalized to account for any matrix effects or instrumental drift, in both low and medium resolution modes. To account for blank contributions from reagents, filters, and sample processing, vials containing only the reagent mixtures or reagents plus unused acid-washed filters were concurrently processed and analyzed, and the resulting “reagent blank” or “process blank” concentrations were subtracted from the final SRM or marine SPM sample concentrations.

Table 2. Minimum determination limits (MDLs; calculated using Micromatter standards) and average PCTE filter blank values for ED-XRF analysis reported as both filter concentration (ng cm^{-2}) and equivalent seawater concentration (pmol L^{-1}) for the average sample filtration volume (8 L).

Analyte	MDL		Filter blank ($n = 11$)	
	(ng cm^{-2})	(pmol L^{-1})	(ng cm^{-2})	(pmol L^{-1})
Al	9.4	540	11.04	63.0
P	2.01	100	BDL	—
Ti	2.52	80	BDL	—
Mn	1.27	40	BDL	—
Fe	0.95	30	2.11	60.0
Ni	0.77	20	BDL	—
Cu	1.25	30	1.31	30.0
Zn	1.28	30	BDL	—

BDL, below detection limit.

Table 3. Results from weekly ED-XRF analysis ($n = 320$) of reference material NIST SRM 2783 (air particulate on filter media) compared to certified values for individual elements (in ng cm^{-2}).

Analyte	Certified value (ng)	± 1 SD	Measured mean value (ng)	± 1 SD	Recovery (%)	\pm Percent
Al	23,210	530	21,400	816	92	3.5
P	n/a	—	1553	99.6	—	—
Ca	13,200	1700	13,330	637	101	4.8
V	48.5	6	BDL	—	—	—
Ti	1490	240	1703	67.1	114	8.9
Mn	320	12	333	8.0	104	2.5
Fe	26,500	1600	28,500	69.2	108	2.6
Ni*	68	12	64	4.5	94	6.5
Cu	404	42	435	20	108	4.9
Zn	1790	130	1524	41.7	85	2.3
Pb	317	54	327	33.9	103	10

BDL, below detection limit; n/a, certified or reference value not available.

*Reference value.

Reference material

Because a certified reference material (CRM) for marine suspended particulate matter is not currently available, NIST SRM 2783 (air particulate on filter media; National Institute of Standards and Technology 2011, hereafter “NIST 2783”) was used to determine analytical precision and accuracy for both methods. Additionally, thin-film secondary standards were prepared on 47 mm diameter, 0.025- μm pore size cellulose ester filters (VSWP MF-Millipore) using 0–3 μm Arizona Test Dust (ATD Powder Technology; Vlasenko et al. 2005). ATD is a natural aerosol material with particle size distribution consistent with marine aerosols (0–3 μm) and is homogenous at a mass as low as 2 mg; it has an elemental composition that includes both lithogenic (e.g., Al and Fe) and anthropogenic (e.g., V and Pb) elements, and is currently being assessed by multiple international labs for use as an aerosol consensus reference material (Morton et al. 2013; Shelley et al. 2015; Buck et al. 2019). ATD samples were prepared by weighing individual ATD subsamples of 2–4 mg into separate acid-washed 15 mL polypropylene centrifuge tubes (Falcon). Immediately before filtration, 5 mL of UHP water was added to the centrifuge tubes and vortexed for 5 s to form a dilute slurry. The slurry was then vacuumed through an acid-washed 0.025 μm MF-Millipore filter (VSWP04700) using a 100-mL Teflon reservoir and filter support (Savillex) installed into a custom-made acrylic vacuum chamber. To transfer any residual ATD material from the centrifuge tube, the tube was rinsed twice more with 5 mL UHP water, vortexed for 5 s, and the rinse solution vacuum filtered with the original slurry. Each 5 mL filtration took less than 20 s, minimizing the solubilization of labile elements from the ATD, and the small pore size was chosen to assure no small particles were able to pass through the filter and escape quantification in the particulate fraction.

Assessment

ED-XRF accuracy, detection limits, and blanks

The minimum detection limit (MDL) for individual elements using ED-XRF is defined as three times the square root of the background intensity measured from a standard of known concentration:

$$\text{MDL} = \frac{(3 * \sqrt{I_b})}{(I_p/c)} \quad (1)$$

where I_b is the background intensity, I_p is the peak intensity, and c is the concentration of the standard (Bertin 2012). MDLs for the ED-XRF method calculated using Eq. 1 and MicroMatter

Table 4. Minimum determination limits (filter blank), average instrument blank values, and average filter blank values for HR ICP-MS analysis reported as both sample concentrations (ppb) and equivalent seawater concentration (pmol L^{-1}) for the average sample filtration volume (8 L).

Analyte	MDL (3xSD; filter blanks)		Instrument blank ($n = 3$)		Filter blank ($n = 5$)	
	(ng g^{-1})	(pmol L^{-1})	(ng g^{-1})	(pmol L^{-1})	(ng g^{-1})	(pmol L^{-1})
Al	3.1	71.1	0.15	2.10	3.1	71.8
P	2.7	53.7	0.50	0.61	3.1	62.7
Ti	3.8	49.6	0.002	0.019	5.3	68.7
Mn	0.04	0.40	0.009	0.060	0.05	0.55
Fe	5.15	57.6	0.25	1.71	3.9	44.2
Ni	1.3	13.4	0.08	0.53	1.3	13.6
Cu	0.06	1.0	0.02	0.10	0.06	0.6
Zn	0.4	4.0	0.17	0.97	0.4	3.8

Table 5. Analysis of certified reference material NIST 1643e (trace elements in natural water) by HR ICP-MS compared to certified values for individual elements (in ppb).

Analyte	Certified value (ppb)	± 1 SD	Measured mean value (ppb)	± 1 SD	Recovery (%)
Al	138.3	8.4	138.2	2.0	100
P	n/a	—	7.0	0.3	—
Ti	n/a	—	0.29	0.03	—
Mn	38.0	0.4	41.0	0.4	108
Fe	95.7	1.4	97.1	2.8	101
Ni	60.9	0.67	56.2	1.0	92
Cu	22.2	0.3	24.4	0.4	110
Zn	76.5	2.1	72.8	1.6	95
Pb	12.10	0.05	9.77	0.28	81

Table 6. Results from HF-assisted microwave digestion and HR ICP-MS analysis ($n = 2$) of NIST SRM 2783 (air particulate on filter media) compared to certified values for individual elements.

Analyte	Certified value (ng)	± 1 SD	Measured mean value (ng)	± 1 SD	Recovery (%)	\pm Percent
Al	23,210	530	26,490	6270	114	27
P	n/a	—	1305	198	—	—
Ti	1490	240	1580	306	106	24
Mn	320	12	377	81	118	25
Fe	26,500	1600	29,990	5970	113	23
Ni*	68	12	136	19	200	28
Cu	404	42	477	102	118	25
Zn	1790	130	1879	382	105	21

n/a, certified or reference value not available.

*italics denote Ni is a Reference value.

standards are shown in Table 2 along with filter blank values for individual elements. For most elements, filter blank values are below the detection limit of the ED-XRF method.

Filter blanks for Al, Fe, and Cu are somewhat higher than the lowest blanks that have previously been reported for polycarbonate filters, although they are generally comparable or lower

Table 7. Orthogonal distance regression statistic; includes outliers removed and RSDs used to calculate SDs for filter digest and ICP-MS methods.

Element	<i>n</i>	Outliers removed	% RSD for ICP-MS	Slope	Slope STD	Slope z-score	Intercept	Intercept STD	Intercept z-score
Al	174	4	5	0.91	0.028	-3.25	0.002	0.052	0.036
P	180	6	6	0.71	0.023	-11.11	-0.69	0.068	-10.2
Ti	189	13	7	0.9	0.059	-1.71	0.14	0.023	6.05
Mn	185	4	6	1	0.19	0.44	0.0055	0.004	1.38
Fe	211	4	5	1.08	0.18	0.48	-0.068	0.11	-0.56
Ni	159	2	9	0.57	0.06	-7.19	0.008	0.002	3.77
Cu	111	0	6	0.083	0.031	-29	0.0079	0.0008	9.11
Zn	91	2	5	0.025	0.0318	-30	0.035	0.002	18

STD, standard deviation.

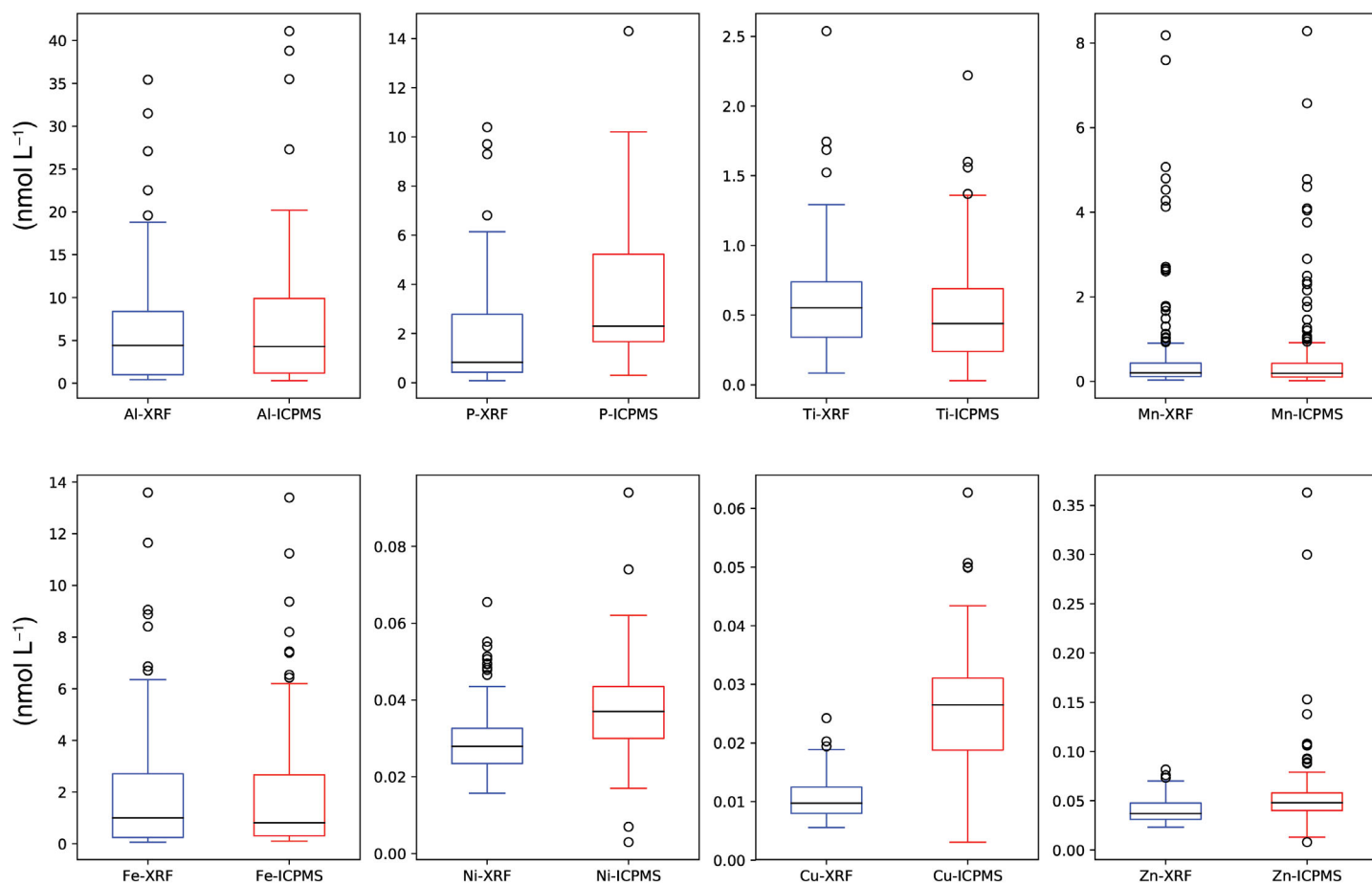


Fig 2. Box and whisker plots of ED-XRF and HR ICP-MS elemental concentrations. Each box represents 50% of data values and is divided at the median. The whiskers represent the upper and lower 99% and the black circles are outliers. Boxplots allow for the comparison of the two methods and represent the median concentrations, spread, and skewness of each analysis. For example, distributions for Al, Mn, and Fe are very similar; examining Cu we note differences in median concentrations and spread.

than reported blanks for other filter types used for SPM sample collection and analysis by HR ICP-MS (e.g., MF-Millipore cellulose filter; Planquette and Sherrell 2012).

NIST 2783 (air particulate on filter media) was used to determine analytical precision and accuracy of the ED-XRF method. Recoveries for individual elements for NIST 2783 by ED-XRF are shown in Table 3. Average ED-XRF values for NIST 2783 are within $\pm 10\%$ of the reported certified value with the exception of Zn (85% of certified value).

HR ICP-MS accuracy, detection limits, and blanks

Detection limits for the HR ICP-MS method calculated from the instrumental blank are shown in Table 4 along with filter blank values for individual elements. NIST certified reference material 1643 (trace elements in natural water) was used to determine analytical accuracy (e.g., instrument selectivity and standards preparation) of the HR ICP-MS method. Recoveries for individual elements for NIST 1643 from HR ICP-MS analysis are shown in Table 5. Efficacy of the digest method was also assessed by digestion and HR ICP-MS analysis of duplicate NIST 2783; recoveries for individual elements are shown in Table 6. Average values for ICP-MS analysis ranged from 102% to 200% (Ni) of the reported certified value. With the exception of Zn, the relative standard deviations (RSDs) of duplicate analysis were all $> 13\%$ and as high as 47% in the case of Ni.

Comparison of ED-XRF and HR ICP-MS paired data

To compare the results of ED-XRF and HR ICP-MS methods, samples across all concentrations, stations, and depths were compared using descriptive statistics (Table 7), boxplots (Fig. 2), and histograms fitted with frequency distributions normalized to 1 (Fig. 3; data can be found in the Supporting Information). Boxplots and histograms were conducted using the Python v2.7.11 SciPy Boxplot and Seaborn packages, respectively. Bin sizes for the histograms were selected using Freedman-Diaconis rule:

$$\text{Bin Size} = 2 * \frac{\text{IQR}(x)}{n^{1/3}} \quad (2)$$

where $\text{IQR}(x)$ is the interquartile range of the data and n is the sample size of x (Freedman and Diaconis 1981). The methods for each analyte were then compared using a Wilcoxon Signed-Ranked Test, a nonparametric test appropriate for comparing oceanic profiles and transects that lack normal and/or symmetric distributions (Sprent 2007; Miller and Miller 2010). Under the null hypothesis, the magnitude of the differences of each sample should be randomly distributed in a symmetric manner around zero ($p > 0.01$; Fig. 4). Results found no evidence of systematic differences between the two methods for Al ($p = 0.043$), Mn ($p = 0.36$), and Fe ($p = 0.71$), but the remaining elements (P, Ti, Ni, Cu, Zn) were all found to be significantly different ($p < 0.00001$ in all cases).

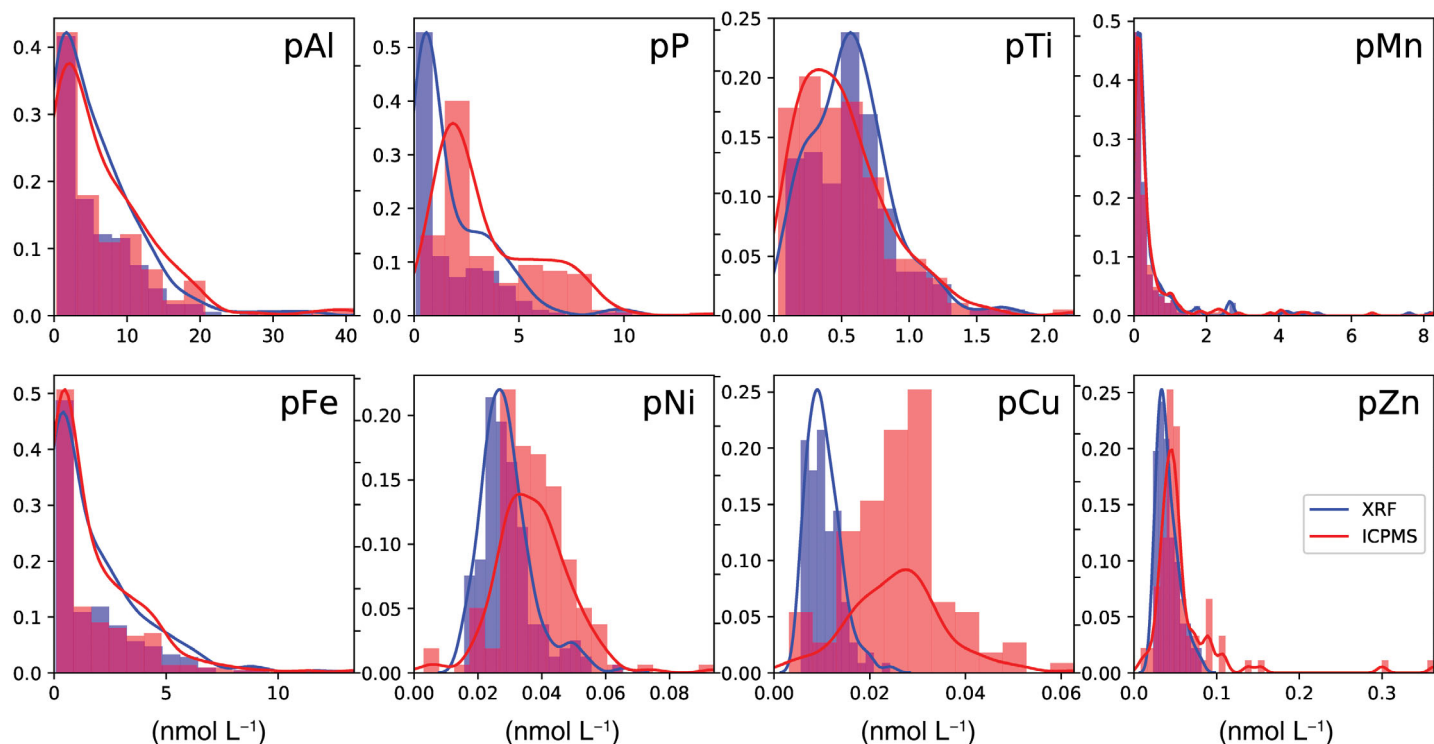


Fig 3. Histograms fitted with density plots (solid lines) for ED-XRF (blue) and HR ICP-MS (red). The height of each bin gives the relative frequency of elemental concentration. Likewise, the peaks of the density plots are the concentrations with the highest frequencies. Al, Mn, and Fe have near identical distributions. ED-XRF values were consistently lower for P, Ni, and Cu when compared to ICP-MS.

A more detailed analysis was conducted using a weighted orthogonal distance regression (WODR), which is an advanced type-II linear regression. WODR is an iterative method used to compare output from two analytical methods that considers error in both the x and y direction. The method provides an estimate of both the slope and intercept with standard errors; is capable of handling data with variable precision (heteroscedastic); is symmetric in that the x - and y - variables can be interchanged and still produce the same results; considers error for both x - and y -data; and does not suffer from the biases generated by inappropriate use of regression (Thompson 1982; Ripley and Thompson 1987; Analytical Methods Committee 1988). WODR analysis was conducted using the Python v2.7.11 SciPy ODR package (Brown and Fuller 1990; Boggs 1992). Random measurement error for the ED-XRF was determined and propagated using the standard deviation (SD) of the slope and intercept of each calibration curve used for analysis as described by Miller and Miller (2010). For the filter digest and ICP-MS method, analytic uncertainty

was estimated using the RSD of repeat measurements ($n = 5$) of three SRMs (BCR-414, ATD, PACS-2) and ranged from 5% to 9% (Table 7).

The statistics generated by the WODR fit are shown in Table 7 and the resultant x - y plots can be found in Fig. 5, where error bars are ± 1 SD. Outliers were identified using Cook's squared distance and removed for WODR estimates (Miller and Miller 2010). To characterize the bias, if any, between the two methods we calculated z -scores using WODR slope (m) and intercept (b) as well as slope standard error ($se[m]$) and intercept standard error estimates ($se[b]$; Table 7). If no bias is present and the results from each method are identical, the WODR slope and intercept estimates would be equal to one and zero, respectively. A z -score represents the number of SDs a slope value is from one or an intercept value is from zero (Miller and Miller 2010). For example, we test the hypothesis that the WODR estimate passes through zero ($H_0: b = 0$) by calculating $z_b = b/se(b)$. Large SD scores (> 3) are an indication of a constant, or translational, bias. Likewise, we

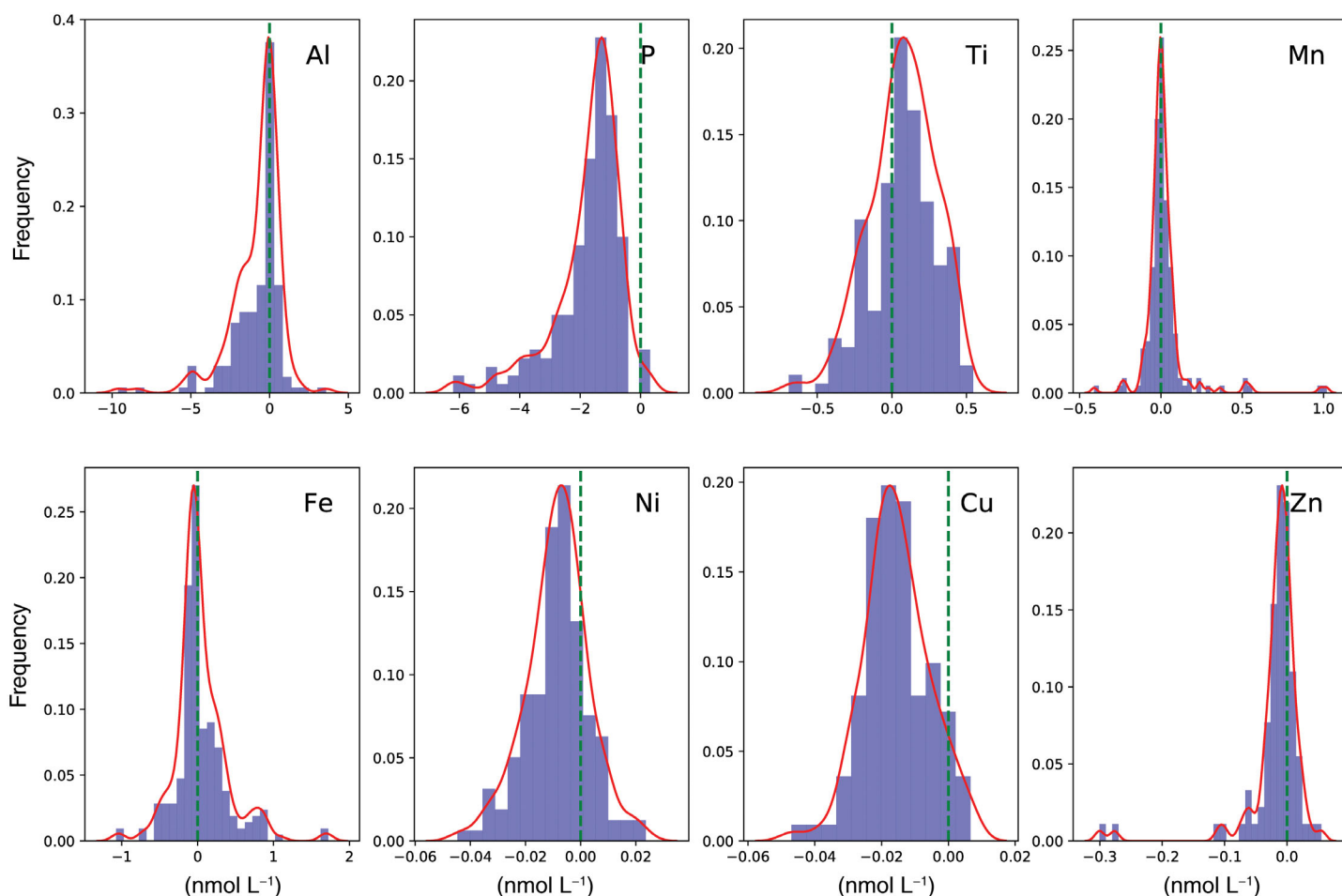


Fig 4. Distributions of (ED-XRF) – (ICP-MS) values used for Wilcoxon signed rank test. If results between the two methods were identical, the differences should be symmetrically distributed around zero. For example, an appraisal of P indicates that ICP-MS analysis was consistently higher when compared to ED-XRF for nearly every sample by 0.5–6 and most frequently by 1.75 nmol L⁻¹.

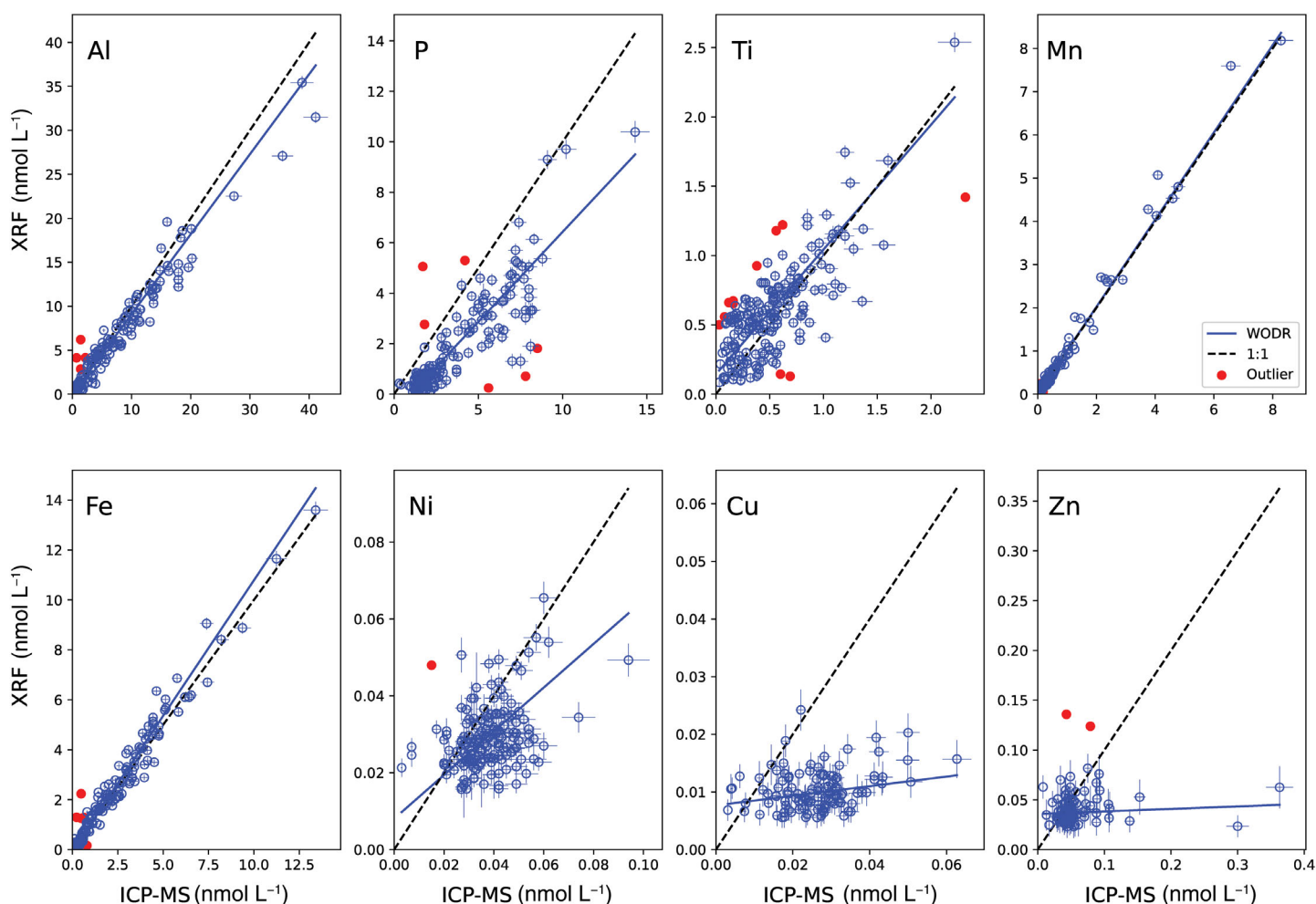


Fig 5. Weighted orthogonal distance regression plots for all data above detection limits. Dash line is 1 : 1; red dots are outliers not used in the calculations; error bars are 1 SD. No statistical difference was found between the two methods for Al, Mn, and Fe; Ti is parallel to but distinct from the $x = y$ line suggesting a methodical bias between the two methods; P has both a constant and variable bias in the intercept and slope, respectively; and Ni, Cu, and Zn have poor agreement between the two methods.

Table 8. ATD results for interlaboratory ICP-MS analysis and ED-XRF.

ATD		ATD XRF $n = 5$						t -test statistics		
Analyte	Labs #	Consensus value (as of April 2020)			Measured value $\mu\text{g g}^{-1}$			Consensus/ ED-XRF	df	p value
		$\mu\text{g g}^{-1}$	± 1 SD	RSD %	value $\mu\text{g g}^{-1}$	± 1 SD	RSD (%)			
Al	11	64,600	8953	13.8	60,000	3460	5.77	1.08	14	0.3
P	7	897	136	15.2	1060	99	9.38	0.85	10	0.05
Ti	9	3330	309	9.28	4040	358	8.87	0.82	12	0.02
Mn	9	761	47	6.18	866	88	10.2	0.88	12	0.02
Fe	11	32,600	2280	6.99	36,000	3330	9.37	0.91	14	0.03
Ni	6	30.7	1.05	3.41	20.8	3.27	15.7	1.48	9	<0.0001*
Cu	7	43.7	0.14	0.32	46.9	8.9	18.9	0.93	10	0.07
Zn	7	101	16.41	16.1	152	12.3	8.09	0.67	10	0.002*

*indicates significant difference between the two methods at $p = 0.01$.

test that the slope of the line is equal to one ($H_0: m = 1$) using $z_m = (m - 1)/se(m)$. Large SDs in this case are evidence of a variable, or rotational, bias.

Examination of the z-score results found no significant difference between the two analytical methods for Mn and Fe, and excellent agreement for Al with a slope z-score slightly higher than three SDs, indicating a small rotational bias resulting from the divergence of values with higher concentrations. For Ti, the WODR line was parallel to but distinct from the $x = y$ line, suggesting a methodical bias between the two methods. The remaining elements (P, Ni, Cu, Zn) had poor agreement on all counts.

Discussion

Our intercomparison study found that ED-XRF can quantify many elements in marine SPM at nanomolar concentrations as accurately and precisely as ICP-MS. While comparisons of Ni, Cu, and Zn between the two methods are poor, this is likely due to the low concentrations found in the Indian Ocean, often at or below the analytical detection limits of both techniques. A similar intercomparison study (Barrett 2015) conducted using a smaller number of samples ($n = 14$) with higher concentrations of Ni (26–52 nmol L⁻¹), Cu (112–495 nmol L⁻¹), and Zn (42–326 nmol L⁻¹) collected from open-ocean surface waters (CLIVAR sections A16N and P2) and a hydrothermal vent field (NE Lau basin) found linear relationships between the two methods for Cu, Ni, and Zn, and results similar to this study where Ni and Zn concentrations were higher when measured by ICP-MS compared to ED-XRF. The consistently higher ICP-MS concentrations found in both studies could be the effect of contamination introduced during the digest process (Bowie et al. 2010; Planquette and Sherrell 2012). Regardless, the current methodologies are inadequate for comparisons of samples near detection limits and further study, using data at higher concentrations, is needed to determine the bias between the two methods. Last, P concentrations also had a constant bias with lower ED-XRF values across the entire concentration range (Figs. 2, 3). This offset is probably not a result of adsorption due to matrix effects caused by overloaded filters as both Al and P were analyzed using the same excitation conditions. Al has a shorter wavelength and would also be similarly affected if the samples did not meet thin-film assumptions. It should be noted Al and P are the lightest elements analyzed for this study and are commonly used as proxies for lithogenic and biogenic endmembers, respectively. Considering a max SPM loading of 1600 μg and sample volumes of 0.5–10 L, and assuming a sample consisting of 100% particulate organic matter with a particulate organic matter : particulate organic carbon (POM : POC) ratio of 0.53 (Lam et al. 2011) and a Redfield C : P ratio of 116 : 1, the upper limit of in situ pP concentrations for ED-XRF analysis would be 0.051–1.22 $\mu\text{mol L}^{-1}$. Likewise, assuming a sample of 100% lithogenic particles and an Al

endmember mass of 7.96% (Wedepohl 1995), the upper limit of in situ pAl concentrations for ED-XRF analysis would be 0.5–9.4 $\mu\text{mol L}^{-1}$. Thus, as long as mass loadings remain below 1600 μg (for a 37 mm filter), ED-XRF analysis is suitable for pAl and pP measurements in most marine systems.

As previously discussed, CRMs for marine suspended particulate matter loaded onto a filter are not commercially available, so NIST 2783 (air particulate on filter media) was used to compare the two methods. As discussed above, a pair of NIST 2783 sample filters is run weekly by ED-XRF for quality assurance purposes; an additional filter set ($n = 2$) was purchased and digested for HR ICP-MS analysis. Open ocean values for SPM concentrations range from 10 to 30 $\mu\text{g L}^{-1}$ with an upper limit of 1000 $\mu\text{g L}^{-1}$ (Ohnemus et al. 2014). NIST 2783 filters have a reported average mass loading of $485 \pm 10 \mu\text{g}$, which is slightly higher than the masses typically collected for SPM samples. To obtain a filter sample with an equivalent mass, volumes of 16–48 L would be needed for typical open ocean SPM concentrations and 0.5 L for the upper limit. Maximum, minimum, and median filter volumes collected for the CLIVAR I09 N effort were 11 L, 5 L, and 10 L, respectively. Elemental concentrations of NIST 2783 for the elements analyzed for this study are all 2–3 orders of magnitude greater than those found in the open ocean (Table 8). However, while NIST 2783 is not a perfect analog for open ocean SPM samples, it can serve as a good indicator of the strengths and weaknesses of each method.

Average ED-XRF values for NIST 2783 are generally within $\pm 10\%$ of the reported certified value. Recovery of Zn falls slightly outside of this range at 85%. Recoveries for most elements certified in NIST 2783 using total digestion and HR ICP-MS were within 102–129% of the reported certified values, confirming results of past studies that found complete dissolution of particulates during the digestion step (Ohnemus et al. 2014). Ni, on the other hand, was the exception, with a concentration double that of the reference value (not certified). While the digestion and HR ICP-MS method reported good accuracy, precision was poor with relative percent difference $[(x_2 - x_1)/((x_2 + x_1)/2)]$, % values ranging from 13% to 24%. There are several possible explanations for this result including: (1) the sample size, or number of replicate samples ($n = 2$), was too small to adequately reflect the bulk average concentrations; (2) of the 2200 filters made by NIST, only 30 were analyzed for homogeneity (2 per each batch of ~ 150); and (3) homogeneity of elemental mass loadings among filters was determined using only one method: instrumental neutron activation analysis (National Institute of Standards and Technology 2011). Unfortunately, the NIST 2783 reference material is no longer available, so follow-up analysis with additional replicates is impossible.

In addition to NIST 2783, five Arizona Test Dust samples (Ultrafine, 0–3 μm particle size) were analyzed by ED-XRF and compared to consensus values reported by 11 other laboratories (Morton et al. 2013; Shelley et al. 2015; Buck et al. 2019).

We recognize the aerosol filter substrate and pore size used to produce the ATD standards is different from the filter type used to collect marine SPM samples for this study. This change was necessary to produce reliable ED-XRF standards of ultrafine ATD. Marine SPM is frequently collected using 0.2–0.45 μm filters; particles smaller than this are considered part of the soluble/colloidal/dissolved size fraction. While operationally defined size classes are an acceptable practice for marine studies, producing an ED-XRF standard requires complete recovery of any filtered material. At the time of this work, the smallest pore-size PCTE filter available was 0.1 μm (Vlasenko et al. 2005 reported a Nuclepore filter with 0.05 μm pore size, which we were unable to find). However, MF-Millipore manufactures a mixed cellulose ester filter with a pore size of 0.025 μm (product #VSWP04700), suitable for near-complete recovery of the entire particle distribution of ATD. Though MF-Millipore filters have higher blank concentrations for all elements except Cu when compared PCTE filters, MF-Millipore filters are suitable for marine SPM collection and analysis as long as the blank correction is <10% the sample concentration (Planquette and Sherrell 2012). Additionally, a similar filter (Whatman 41) has been employed successfully for complementary marine aerosol studies (Morton et al. 2013; Shelley et al. 2015; Marsay et al. 2018; Buck et al. 2019). The use of the small pore-size MF-Millipore filter proved appropriate, as the ED-XRF analysis of the filter-loaded ATD showed no statistical difference for six of the eight elements (t -test; $p = 0.01$; Table 8) when compared to ICP-MS results of ATD powder digested and analyzed by 11 independent labs (the exceptions were Ni, which reported 68% less the consensus value, and Zn, which reported 50% more). Furthermore, ED-XRF had satisfactory precision with element-specific RSD trends that ranged from 6% to 19% and agreed with interlaboratory variability of ATD as determined by HR ICP-MS.

The analysis of SPM by ED-XRF has many advantages and can serve as an independent analytical method for marine SPM or as a complementary technique to expand the suite of elements analyzed by other methods or instrumentation. ED-XRF requires little sample preparation and processing, which offers high throughput: for example, 100 samples can easily be analyzed for multiple bioactive elements in 1 week. Additionally, ED-XRF techniques are cost effective and nondestructive and do not require a digestion step: eliminating both the use of hazardous acid digestions and the risk of contamination and uncertainties associated with extensive sample handling and processing required by total digestion methods (Planquette and Sherrell 2012; Ohnemus et al. 2014). Thus, bulk analysis of SPM by ED-XRF can advance the GEOTRACES directive by addressing challenges related to: intercalibration between laboratories, cruises, and crossover stations; the development of SPM consensus material for quality assurance and quality control such as those developed for dissolved species (like SAFE and GEOTRACES); and sample archival of analyzed filters for future use (Henderson and Marchal 2015).

Currently, ED-XRF methods are restricted by detection limits for trace elements found in low levels in the particulate phase due to a combination of low overall particulate concentrations in the marine environment and small filter volumes used (< 5 L). This is particularly true for Cu, Ni, and Zn as 100, 52, and 120 samples were below study ED-XRF detection limits, respectively. Furthermore, ED-XRF cannot be used to analyze marine SPM collected onto polyethersulfone filters, which have been employed in sample collection for their high loading capacity, due to artifacts produced by the high sulfur content during ED-XRF analysis. However, these limitations can be resolved with further methodological refinement or addressed with shipboard sampling strategies that produce higher filtration volumes on appropriate filter types. It should be noted that cellulose ester filters have been proven successful for the collection and analysis of marine SPM by HR ICP-MS (Planquette and Sherrell 2012) and now by ED-XRF.

Recommendations

First, we recommend improving ED-XRF detection limits for elements with sub-nanomolar SPM concentrations found in the open ocean. For this study, minimum determination limits were improved for Fe and Mn by creating low concentration calibration standards using the DDTC precipitate method. Similar calibrants should be created for elements such as Cu, Ni, Zn, and Pb. In a promising new method, Yarkin et al. (2018) created low mass, low concentration (ng cm^{-2}) multielement standards on filters using a desolvating nebulizer. A follow-up intercalibration study conducted by Hyslop et al. (2019) involving eight laboratories using ED-XRF and ICP-MS found these standards to be sufficient for ED-XRF calibration for Na, Al, Si, S, K, Ti, V, Mn, Fe, Co, Ni, Se, As, and Pb. Such standards are required as commercially available calibrants are uncommon and those that are available have particulate masses and elemental concentrations much higher than is typical of SPM in most of the ocean.

Second, advances in XRF instrumentation, technology, and techniques over the past decade should be exploited. For example, commercially available silicon drift detectors (SDDs) have better energy resolution and higher count rates, lower signal-to-noise ratios, and thus lower detection limits than the Si(Li) detector used for this study. Thermo Fisher Scientific's most recent generation of SDD, the SDD¹⁰⁰⁰, has double the active surface area, an improved preamplifier, and a larger detection window, allowing for the capture of more fluorescent radiation, thus improving sensitivity by at least a factor of 2 for all elements. Higher count rates also result in shorter measurement times improving throughput.

Also, total reflection X-ray fluorescence (TXRF) instruments are becoming readily available on the commercial market and have promise for quantitative SPM analysis with extremely low detection limits (Bohlen and Klockenkämper 2015). TXRF, a high-performance variant of traditional ED-XRF methods, is

based on a unique geometric setup between X-ray tube, sample, and detector. In TXRF, the sample is irradiated at a very shallow (or grazing) angle of 0.1° , and the resulting fluorescence signal is collected by a detector located at 90° relative to the sample surface (in ED-XRF the X-ray tube and detector are positioned at about 40° relative to the sample). Such a configuration reduces spectral background signals (filter matrix), resulting in extremely low detection limits. TXRF methodologies have been increasingly used to quantify pollution levels in air, water, and soil (see review, Bilo et al. 2018). In a compelling study by Bontempi et al. (2010), direct analysis of elemental concentrations of aerosols deposited onto filters in the urban Italian area of Brescia were analyzed and methodologies reported low ng cm^{-2} detection limits. While methods for the marine environment have yet to be developed, TXRF may be an option for low-level analysis of marine SPM and perhaps even dissolved metals and aerosols.

Last, we propose creating a series of reference materials on PCTE or MF-Millipore filters with elemental ratios analogous to atmospheric, fluvial, hydrothermal, and autochthonous sources. While the current effort to create and distribute ATD (Morton et al. 2013) is a good start, a much larger effort is needed. Such reference materials are currently unavailable but are paramount for methodological quality assurance and analytical accuracy (Shelley et al. 2015) as demonstrated by the creation and use of SAFE and GEOTRACES standards for dissolved elements (Johnson et al. 2007). Furthermore, by preparing consensus reference materials on PCTE or MF-Millipore filters, particle quantification by nondestructive methods (such as ED-XRF) could be conducted before distribution to laboratories that utilize digestions, advancing intercalibration efforts for GEOTRACES, and other international oceanographic programs.

References

- Analytical Methods Committee. 1988. Uses (proper and improper) of correlation-coefficients. *Analyst* **113**: 1469–1471. doi:10.1039/AN9881301469
- Anderson, R. F., and C. T. Hayes. 2015. Characterizing marine particles and their impact on biogeochemical cycles in the GEOTRACES program. *Prog. Oceanogr.* **133**: 1–5. doi:10.1016/j.pocean.2014.11.010
- Baker, E. T. 1976. Distribution, composition, and transport of suspended particulate matter in vicinity of Willapa Submarine Canyon, Washington. *Geol. Soc. Am. Bull.* **87**: 625–632. doi:10.1130/0016-7606(1976)87<625:DCATOS>2.0.CO;2
- Baker, E. T., and D. Z. Piper. 1976. Suspended particulate matter - collection by pressure filtration and elemental analysis by thin-film X-ray-fluorescence. *Deep-Sea Res.* **23**: 181–186. doi:10.1016/S0011-7471(76)80027-7
- Barrett, P. M. 2015. The biogeochemistry of particulate trace elements and isotopes in the North Atlantic Ocean. Ph.D. thesis. Univ. of Washington.
- Barrett, P. M., J. A. Resing, N. J. Buck, C. S. Buck, W. M. Landing, and C. I. Measures. 2012. The trace element composition of suspended particulate matter in the upper 1000 m of the eastern North Atlantic Ocean: A16N. *Mar. Chem.* **142**: 41–53. doi:10.1016/j.marchem.2012.07.006
- Barrett, P. M., J. A. Resing, N. J. Buck, W. M. Landing, P. L. Morton, and R. U. Shelley. 2015. Changes in the distribution of Al and particulate Fe along A16N in the eastern North Atlantic Ocean between 2003 and 2013: Implications for changes in dust deposition. *Mar. Chem.* **177**: 57–68. doi:10.1016/j.marchem.2015.02.009
- Barrett, P. M., J. A. Resing, M. M. Grand, C. I. Measures, and W. M. Landing. 2018. Trace element composition of suspended particulate matter along three meridional CLIVAR sections in the Indian and Southern oceans: Impact of scavenging on Al distributions. *Chem. Geol.* **502**: 15–28. doi:10.1016/j.chemgeo.2018.06.015
- Bertin, E. P. 2012. Principles and practice of X-ray spectrometric analysis. Springer Science & Business Media.
- Bilo, F., and others. 2018. Comparison of multiple X-ray fluorescence techniques for elemental analysis of particulate matter collected on air filters. *J. Aerosol Sci.* **122**: 1–10. doi:10.1016/j.jaerosci.2018.05.003
- Boggs, P. 1992. User's reference guide for ODRPACK version 2.01 software for weighted orthogonal distance regression.
- Bohlen, A. V., and R. Klockenkämper. 2015. Total-reflection X-ray fluorescence analysis and related methods, 2nd Edition. Wiley.
- Bontempi, E., and others. 2010. Total reflection X-ray fluorescence (TXRF) for direct analysis of aerosol particle samples. *Environ. Technol.* **31**: 467–477. doi:10.1080/09593330903513260
- Bowie, A. R., A. T. Townsend, D. Lannuzel, T. A. Remenyi, and P. van der Merwe. 2010. Modern sampling and analytical methods for the determination of trace elements in marine particulate material using magnetic sector inductively coupled plasma-mass spectrometry. *Anal. Chim. Acta* **676**: 15–27. doi:10.1016/j.aca.2010.07.037
- Brown, P. J. and W. E. Fuller [eds.] 1990. Statistical analysis of measurement error models and applications. *In* Proceedings of the AMS-IMS-SIAM joint summer research conference held June 10–16, 1989, with support from the National Science Foundation and the U.S. Army Research Office. American Mathematical Society.
- Buck, C. S., W. M. Landing, and J. A. Resing. 2010a. Particle size and aerosol iron solubility: A high-resolution analysis of Atlantic aerosols. *Mar. Chem.* **120**: 14–24. doi:10.1016/j.marchem.2008.11.002
- Buck, C. S., W. M. Landing, J. A. Resing, and C. I. Measures. 2010b. The solubility and deposition of aerosol Fe and other trace elements in the North Atlantic Ocean: Observations from the A16N CLIVAR/CO₂ repeat hydrography section. *Mar. Chem.* **120**: 57–70.
- Buck, C. S., W. M. Landing, and J. Resing. 2013. Pacific Ocean aerosols: Deposition and solubility of iron, aluminum, and

- other trace elements. *Mar. Chem.* **157**: 117–130. doi:[10.1016/j.marchem.2013.09.005](https://doi.org/10.1016/j.marchem.2013.09.005)
- Buck, C. S., A. Aguilar-Islas, C. Marsay, D. Kadko, and W. M. Landing. 2019. Trace element concentrations, elemental ratios, and enrichment factors observed in aerosol samples collected during the US GEOTRACES eastern Pacific Ocean transect (GP16). *Chem. Geol.* **511**: 212–224. doi:[10.1016/j.chemgeo.2019.01.002](https://doi.org/10.1016/j.chemgeo.2019.01.002)
- Cullen, J. T., and R. M. Sherrell. 1999. Techniques for determination of trace metals in small samples of size-fractionated particulate matter: Phytoplankton metals off central California. *Mar. Chem.* **67**: 233–247. doi:[10.1016/S0304-4203\(99\)00060-2](https://doi.org/10.1016/S0304-4203(99)00060-2)
- Cullen, J. T., M. P. Field, and R. M. Sherrell. 2001. Determination of trace elements in filtered suspended marine particulate material by sector field HR-ICP-MS. *J. Anal. At. Spectrom.* **16**: 1307–1312. doi:[10.1039/b104398f](https://doi.org/10.1039/b104398f)
- Eggemann, D. W., and P. R. Betzer. 1976. Decomposition and analysis of refractory oceanic suspended materials. *Anal. Chem.* **48**: 886–890. doi:[10.1021/ac60370a005](https://doi.org/10.1021/ac60370a005)
- Ellis, A. T. 2001. Energy-dispersive X-ray fluorescence analysis using X-ray tube excitation, p. 218–257. *In* R. E. Van Grieken and A. A. Markowicz [eds.], *Handbook of X-ray spectrometry*, 2nd ed. CRC Press.
- European Commission. 2017. Certified reference material BCR-414 – plankton, revised. Community Bureau of Reference, Joint Research Centre.
- Feely, R., G. Massoth, and G. Lebon. 1991. Sampling of marine particulate matter and analysis by X-ray fluorescence spectrometry. *In* D. C. Hurd and D. W. Spencer [eds.], *Marine particles: Analysis and characterization*, v. **63**. American Geophysical Union.
- Feely, R. A., M. Lewison, G. J. Massoth, G. Robert-Baldo, J. W. Lavelle, R. H. Byrne, K. L. Von Damm, and H. C. Curl Jr. 1987. Composition and dissolution of black smoker particulates from active vents on the Juan-de-Fuca Ridge. *J. Geophys. Res. Solid Earth* **92**: 11347–11363. doi:[10.1029/JB092iB11p11347](https://doi.org/10.1029/JB092iB11p11347)
- Feely, R. A., J. H. Trefry, G. T. Lebon, and C. R. German. 1998. The relationship between P/Fe and V/Fe ratios in hydrothermal precipitates and dissolved phosphate in seawater. *Geophys. Res. Lett.* **25**: 2253–2256. doi:[10.1029/98GL01546](https://doi.org/10.1029/98GL01546)
- Freedman, D., and P. Diaconis. 1981. On the histogram as a density estimator - L2 theory. *Z. Wahrscheinlichkeitstheorie Verwandte Geb.* **57**: 453–476.
- Henderson, G. M., and O. Marchal. 2015. Recommendations for future measurement and modelling of particles in GEOTRACES and other ocean biogeochemistry programmes. *Prog. Oceanogr.* **133**: 73–78. doi:[10.1016/j.poccean.2015.01.015](https://doi.org/10.1016/j.poccean.2015.01.015)
- Ho, T. Y., W. C. Chou, H. L. Lin, and D. D. Sheu. 2011. Trace metal cycling in the deep water of the South China Sea: The composition, sources, and fluxes of sinking particles. *Limnol. Oceanogr.* **56**: 1225–1243. doi:[10.4319/lo.2011.56.4.1225](https://doi.org/10.4319/lo.2011.56.4.1225)
- Holmes, G. S. 1981. The limitations of accurate thin-film X-ray-fluorescence analysis of natural particulate matter - problems and solutions. *Chem. Geol.* **33**: 333–353. doi:[10.1016/0009-2541\(81\)90107-8](https://doi.org/10.1016/0009-2541(81)90107-8)
- Holynska, B., and K. Bisiniek. 1976. Determination of trace amounts of metals in saline water by energy dispersive XRF using NADDTc preconcentration. *J. Radioanal. Chem.* **31**: 159–166. doi:[10.1007/BF02516475](https://doi.org/10.1007/BF02516475)
- Hyslop, N. P., and others. 2019. An inter-laboratory evaluation of new multi-element reference materials for atmospheric particulate matter measurements. *Aerosol Sci. Technol.* **53**: 771–782. doi:[10.1080/02786826.2019.1606413](https://doi.org/10.1080/02786826.2019.1606413)
- Jeandel, C., M. Rutgers van der Loeff, P. J. Lam, M. Roy-Barman, R. M. Sherrell, S. Kretschmer, C. German, and F. Dehairs. 2015. What did we learn about ocean particle dynamics in the GEOSECS–JGOFS era? *Prog. Oceanogr.* **133**: 6–16. doi:[10.1016/j.poccean.2014.12.018](https://doi.org/10.1016/j.poccean.2014.12.018)
- Johnson, K. S., and others. 2007. Developing standards for dissolved iron in seawater. *EOS Trans. AGU* **88**: 131–132. doi:[10.1029/2007EO110003](https://doi.org/10.1029/2007EO110003)
- Krachler, M. 2007. Environmental applications of single collector high resolution ICP-MS. *J. Environ. Monitor.* **9**: 790–804. doi:[10.1039/b703823m](https://doi.org/10.1039/b703823m)
- Kurfurst, U. 1991. Statistical treatment of ETA-AAS (electrothermal atomisation - atomic absorption spectrometry) solid sampling data of heterogeneous samples. *Pure Appl. Chem.* **63**: 1205–1211. doi:[10.1351/pac199163091205](https://doi.org/10.1351/pac199163091205)
- Kurfurst, U., J. Pauwels, K. H. Grobecker, M. Stoeppler, and H. Muntau. 1993. Microheterogeneity of trace-elements in reference materials - determination and statistical evaluation. *Fresenius J. Anal. Chem.* **345**: 112–120. doi:[10.1007/BF00322568](https://doi.org/10.1007/BF00322568)
- Lam, P. J., S. C. Doney, and J. K. B. Bishop. 2011. The dynamic ocean biological pump: Insights from a global compilation of particulate organic carbon, CaCO₃, and opal concentration profiles from the mesopelagic. *Global Biogeochem. Cycles* **25**: GB3009. doi:[10.1029/2010GB003868](https://doi.org/10.1029/2010GB003868)
- Lam, P. J., B. S. Twining, C. Jeandel, A. Roychoudhury, J. A. Resing, P. H. Santschi, and R. F. Anderson. 2015. Methods for analyzing the concentration and speciation of major and trace elements in marine particles. *Prog. Oceanogr.* **133**: 32–42. doi:[10.1016/j.poccean.2015.01.005](https://doi.org/10.1016/j.poccean.2015.01.005)
- Lamborg, C. H., K. O. Buesseler, and P. J. Lam. 2008a. Sinking fluxes of minor and trace elements in the North Pacific Ocean measured during the VERTIGO program. *Deep-Sea Res. II Top. Stud. Oceanogr.* **55**: 1564–1577. doi:[10.1016/j.dsr2.2008.04.012](https://doi.org/10.1016/j.dsr2.2008.04.012)
- Lamborg, C. H., and others. 2008b. The flux of bio- and lithogenic material associated with sinking particles in the mesopelagic "twilight zone" of the northwest and North Central Pacific Ocean. *Deep-Sea Res. II Top. Stud. Oceanogr.* **55**: 1540–1563. doi:[10.1016/j.dsr2.2008.04.011](https://doi.org/10.1016/j.dsr2.2008.04.011)
- Marsay, C. M., P. J. Lam, M. I. Heller, J.-M. Lee, and S. G. John. 2018. Distribution and isotopic signature of ligand-

- leachable particulate iron along the GEOTRACES GP16 East Pacific Zonal Transect. *Mar. Chem.* **201**: 198–211. doi:[10.1016/j.marchem.2017.07.003](https://doi.org/10.1016/j.marchem.2017.07.003)
- Measures, C. I., W. M. Landing, M. T. Brown, and C. S. Buck. 2008. A commercially available rosette system for trace metal-clean sampling. *Limnol. Oceanogr.: Methods* **6**: 384–394. doi:[10.4319/lom.2008.6.384](https://doi.org/10.4319/lom.2008.6.384)
- Miller, J. N., and J. C. Miller. 2010. *Statistics and chemometrics for analytical chemistry*. Prentice Hall.
- Morton, P. L., and others. 2013. Methods for the sampling and analysis of marine aerosols: Results from the 2008 GEOTRACES aerosol intercalibration experiment. *Limnol. Oceanogr.: Methods* **11**: 62–78. doi:[10.4319/lom.2013.11.62](https://doi.org/10.4319/lom.2013.11.62)
- Morton, P. L., and others. 2019. Shelf inputs and lateral transport of Mn, Co, and Ce in the western North Pacific Ocean. *Front. Mar. Sci.* **6**: 591. doi:[10.3389/fmars.2019.00591](https://doi.org/10.3389/fmars.2019.00591)
- National Institute of Standards & Technology. 2011. Standard reference material 2783 – Air particulate on filter media. Available from https://www-s.nist.gov/srmors/view_detail.cfm?srm=2783 [accessed January 2015].
- National Research Council of Canada. 1997. Certified reference material PACS-2 – marine sediment reference materials for trace metals and other constituents. Available from <https://nrc.canada.ca/en/certifications-evaluations-standards/certified-reference-materials> [accessed January 2015].
- Ohnemus, D. C., M. E. Auro, R. M. Sherrell, M. Lagerström, P. L. Morton, B. S. Twining, S. Rauschenberg, and P. J. Lam. 2014. Laboratory intercomparison of marine particulate digestions including piranha: A novel chemical method for dissolution of polyethersulfone filters. *Limnol. Oceanogr.: Methods* **12**: 530–547. doi:[10.4319/lom.2014.12.530](https://doi.org/10.4319/lom.2014.12.530)
- Ohnemus, D. C., and P. J. Lam. 2015. Cycling of lithogenic marine particles in the US GEOTRACES North Atlantic transect. *Deep-Sea Res. II Top. Stud. Oceanogr.* **116**: 283–302. doi:[10.1016/j.dsr2.2014.11.019](https://doi.org/10.1016/j.dsr2.2014.11.019)
- Pauwels, J., and C. Vandecasteele. 1993. Determination of the minimum sample mass of a solid CRM to be used in chemical-analysis. *Fresenius J. Anal. Chem.* **345**: 121–123. doi:[10.1007/BF00322569](https://doi.org/10.1007/BF00322569)
- Planquette, H., and R. M. Sherrell. 2012. Sampling for particulate trace element determination using water sampling bottles: Methodology and comparison to in situ pumps. *Limnol. Oceanogr.: Methods* **10**: 367–388. doi:[10.4319/lom.2012.10.367](https://doi.org/10.4319/lom.2012.10.367)
- Quisefit, J. P., P. Dechateaubourg, S. Garivait, and E. Steiner. 1994. Quantitative analyses of aerosol filters by wavelength-dispersive X-ray spectrometry from bulk reference samples. *X-Ray Spectrom.* **23**: 59–64. doi:[10.1002/xrs.1300230204](https://doi.org/10.1002/xrs.1300230204)
- Resing, J. A., E. T. Baker, J. E. Lupton, S. L. Walker, D. A. Butterfield, G. J. Massoth, and K. Nakamura. 2009. Chemistry of hydrothermal plumes above submarine volcanoes of the Mariana Arc. *Geochem. Geophys. Geosyst.* **10**: Q02009. doi:[10.1029/2008GC002141](https://doi.org/10.1029/2008GC002141)
- Ripley, B. D., and M. Thompson. 1987. Regression techniques for the detection of analytical bias. *Analyst* **112**: 377–383. doi:[10.1039/an9871200377](https://doi.org/10.1039/an9871200377)
- Shelley, R. U., P. L. Morton, and W. M. Landing. 2015. Elemental ratios and enrichment factors in aerosols from the US-GEOTRACES North Atlantic transects. *Deep-Sea Res. II Top. Stud. Oceanogr.* **116**: 262–272. doi:[10.1016/j.dsr2.2014.12.005](https://doi.org/10.1016/j.dsr2.2014.12.005)
- Sprent, P. 2007. Applied nonparametric statistical methods, p. 125–149. *In* P. Sprent and N. C. Smeeton [eds.], *Applied nonparametric statistical methods*, 4th ed. Chapman & Hall.
- Thompson, M. 1982. Regression methods in the comparison of accuracy. *Analyst* **107**: 1169–1180. doi:[10.1039/an9820701169](https://doi.org/10.1039/an9820701169)
- Twining, B. S., S. Rauschenberg, P. L. Morton, D. C. Ohnemus, and P. J. Lam. 2015. Comparison of particulate trace element concentrations in the North Atlantic Ocean as determined with discrete bottle sampling and in situ pumping. *Deep-Sea Res. II Top. Stud. Oceanogr.* **116**: 273–282. doi:[10.1016/j.dsr2.2014.11.005](https://doi.org/10.1016/j.dsr2.2014.11.005)
- Vlasenko, A., S. Sjögren, E. Weingartner, H. W. Gäggeler, and M. Ammann. 2005. Generation of submicron Arizona test dust aerosol: Chemical and hygroscopic properties. *Aerosol Sci. Technol.* **39**: 452–460. doi:[10.1080/027868290959870](https://doi.org/10.1080/027868290959870)
- Wedepohl, K. H. 1995. The composition of the continental crust. *Geochim. Cosmochim. Acta* **59**: 1217–1232. doi:[10.1016/0016-7037\(95\)00038-2](https://doi.org/10.1016/0016-7037(95)00038-2)
- Yatkin, S., K. Trzepla, W. H. White, and N. P. Hyslop. 2018. Generation of multi-element reference materials on PTFE filters mimicking ambient aerosol characteristics. *Atmos. Environ.* **189**: 41–49. doi:[10.1016/j.atmosenv.2018.06.034](https://doi.org/10.1016/j.atmosenv.2018.06.034)

Acknowledgments

This work was funded by NSF-OCE-0649639 to WML and NSF-OCE-1237011 to JAR. Funding was also provided by the Joint Institute for the Study of the Atmosphere and Ocean (JISAO) under NOAA Cooperative Agreement NA15OAR4320063, Contribution No. 2020-1077. A portion of this work was completed by PLM at the National High Magnetic Field Laboratory, which is supported by the National Science Foundation through DMR-1644779 and the State of Florida. We thank: Kati Gosnell, Mariko Hatta, and Bill Hiscock for trace metal sampling; REU Rachel Weisend for help with the sample digestions (FSU); the captain and crew of the R/V *Revelle* for their technical support during the CLIVAR I09N cruise; R. Wigham S. Bigley, and J. Beeson for review and editing support; and two anonymous reviewers for comments.

Conflict of Interest

None declared.

Submitted 13 August 2020

Revised 13 April 2021

Accepted 18 April 2021

Associate editor: Gregory Cutter